

Higher Dimensional Conformal- $U(1)$ Gauge/Gravity Black Holes: Thermodynamics and Quasinormal Modes

Seyed Hossein Hendi^{1,2*}, Mehrab Momennia^{1†} and Fatemeh Soltani Bidgoli¹

¹ *Physics Department and Biruni Observatory,*

College of Sciences, Shiraz University, Shiraz 71454, Iran

² *Research Institute for Astronomy and Astrophysics of Maragha (RIAAM), P.O. Box 55134-441, Maragha, Iran*

Motivated by quantum nature of gravitating black holes, higher dimensional exact solutions of conformal gravity with an abelian gauge field is obtained. It is shown that the obtained solutions can be interpreted as singular black holes. Then, we calculate the conserved and thermodynamic quantities, and also, perform thermal stability analysis of the obtained black hole solutions. In addition, we show that the critical behavior does not occur for these black holes. Finally, we consider a minimally coupled massive scalar perturbation and calculate the quasinormal modes by using the sixth order WKB approximation and the asymptotic iteration method. We also investigate the time evolution of modes through the discretization scheme.

I. INTRODUCTION

Considering the quantum effects in gravitational interaction, one may find that the higher-curvature modification of general relativity is inevitable. However, in order to have a physically ghost free theory of higher-curvature modifications, some special constraints should be applied. Fortunately, there are known higher-curvature interesting renormalizable actions with no ghosts under certain criterion. As an interesting example, we can regard the so-called Conformal Gravity (CG), which is defined by the square of the Weyl tensor [1, 2].

The CG is an interesting theory of modified general relativity with a remarkable property which is sensitive to angles, but not distances. In other words, it is invariant under local stretching of the metric which is called the Weyl transformation, $g_{\mu\nu}(x) \rightarrow \Omega^2(x)g_{\mu\nu}(x)$. It has been shown that CG is useful for constructing supergravity theories [3, 4] and can be considered as a possible UV completion of gravity [5–7]. It may be also arisen from twister-string theory with both closed strings and gauge-singlet open strings [8]. Moreover, CG can be appeared as a counterterm in

* email address: hendi@shirazu.ac.ir

† email address: m.momennia@shirazu.ac.ir

*adS*₅/*CFT*₄ calculations [9, 10]. In addition to the motivations mentioned above, solving the dark matter and dark energy problems are two of the most important and interesting motivations of studying CG theory [7].

Since CG is renormalizable [5, 11] and the requirement of conformal invariance at the classical level leads to a renormalizable gauge theory of gravity, it seems interesting to consider black holes in CG which permits a consistent picture of black hole evaporation [12]. The first attempt to obtain the spherically symmetric black hole solutions in four dimensions has been done by Bach [13], and then, Buchdahl has considered a particular case of the conformal solutions in [14]. It is worthwhile to mention that the 4-dimensional solution of Einstein gravity is a solution of CG as well. In addition, it has been shown that the Einstein solutions can be obtained by considering suitable boundary condition on the metric in CG [15, 16].

CG can also be introduced in higher dimensions ($D > 4$), straightforwardly [17]. Nevertheless, unlike the 4-dimensional case, CG does not admit Einstein trivial solutions in higher dimensions. This nontrivial behavior is due to the fact that in contrast to the 4-dimensional action, the Kretschmann scalar $R^{\alpha\beta\gamma\delta}R_{\alpha\beta\gamma\delta}$ contributes dynamically in the higher dimensions [18]. Such a nontrivial behavior motivates one to investigate higher dimensional CG black hole solutions.

On the other hand, when a black hole undergoes perturbations, the resulting behavior leads to some oscillations which are called quasinormal modes (QNMs). The quasinormal frequencies (QNMs) related to such QNMs are independent of initial perturbations and they are the intrinsic imprint of the black hole response to external perturbations on the background spacetime of black hole. The asymptotic behavior of the QNMs relates to the quantum gravity [19, 20] and the imaginary part of the frequencies in adS spacetime corresponds to the decay of perturbations of a thermal state in the conformal field theory [21, 22].

The QNM is one of the most important and exciting features of compact objects and describes the evolution of fields on the background spacetime of such objects [23–25]. Therefore, the QNM spectrum reflects the properties of spacetime, and consequently, we can find out about the properties of background spacetime by studying the QNMs. As a result, the QNM spectrum will be a function of black hole parameters, such as mass, charge, and angular momentum. The QNM spectrum of gravitational perturbations can be observed by gravitational wave detectors [26–28], and after the detection of the QNMs of compact binary mergers by LIGO, investigation of the QNMs of black holes attracted attention during the past three years (for instance, see an incomplete list [29–44] and references therein). In this paper, we consider higher dimensional charged black hole solutions in CG theory and investigate their stabilities.

The outline of this paper is as follows. In the next section, we give a brief review on neutral and charged black holes of CG in 4-dimensional spacetime. We also construct D -dimensional topological static black hole solutions of CG gravity in the presence of generalized Maxwell theory. Then, the thermodynamics of obtained solutions is investigated and the conserved and thermodynamic quantities are calculated. We also perform the thermal stability analysis of the solutions in the canonical ensemble, and also, by using geometrical thermodynamic approach. In addition, we investigate the possibility of the critical behavior of obtained black hole solutions. Finally, we consider a minimally coupled massive scalar perturbation in the background spacetime of the black holes and calculate the related QNMs by using the sixth order WKB approximation and the asymptotic iteration method (AIM). Then, we argue that these black holes cannot have quasi-resonance modes which are a feature of massive scalar perturbations. We finish our paper with some concluding remarks.

II. FOUR-DIMENSIONAL EXACT SOLUTIONS

At the first step, we consider a four-dimensional conformal action as

$$\begin{aligned} I_G &= -\alpha \int d^4x \sqrt{-g} C_{\lambda\mu\nu\kappa} C^{\lambda\mu\nu\kappa} \\ &\equiv -2\alpha \int d^4x \sqrt{-g} \left[R^{\mu\nu} R_{\mu\nu} - \frac{1}{3} (R^\alpha_\alpha)^2 \right], \end{aligned} \quad (1)$$

where the Weyl conformal tensor is

$$\begin{aligned} C_{\lambda\mu\nu\kappa} &= R_{\lambda\mu\nu\kappa} + \frac{1}{6} R^\alpha_\alpha [g_{\lambda\nu} g_{\mu\kappa} - g_{\lambda\kappa} g_{\mu\nu}] \\ &\quad - \frac{1}{2} [g_{\lambda\nu} R_{\mu\kappa} - g_{\lambda\kappa} R_{\mu\nu} - g_{\mu\nu} R_{\lambda\kappa} + g_{\mu\kappa} R_{\lambda\nu}]. \end{aligned} \quad (2)$$

Variation of action (1) with respect to the metric tensor leads to the following equation of motion

$$\begin{aligned} W^{\mu\nu} &= 2C^{\mu\lambda\nu\kappa}_{;\lambda\kappa} - C^{\mu\lambda\nu\kappa} R_{\lambda\kappa} = \\ &\frac{1}{2} g^{\mu\nu} (R^\alpha_\alpha)^{;\beta}_{;\beta} + R^{\mu\nu;\beta}_{;\beta} - R^{\mu\beta;\nu}_{;\beta} - R^{\nu\beta;\mu}_{;\beta} - 2R^{\mu\beta} R^\nu_\beta \\ &+ \frac{1}{2} g^{\mu\nu} R_{\alpha\beta} R^{\alpha\beta} - \frac{2}{3} g^{\mu\nu} (R^\alpha_\alpha)^{;\beta}_{;\beta} + \frac{2}{3} (R^\alpha_\alpha)^{;\mu;\nu} + \frac{2}{3} R^\alpha_\alpha R^{\mu\nu} - \frac{1}{6} g^{\mu\nu} (R^\alpha_\alpha)^2 = 0. \end{aligned} \quad (3)$$

It was shown that the static spherically symmetric solution of conformal gravity in four dimensions can be written as

$$ds^2 = -f(r) dt^2 + \frac{dr^2}{f(r)} + r^2 d\Omega^2, \quad (4)$$

where $d\Omega^2$ is the line element of a 2-sphere, S^2 , and the metric function is [14]

$$f(r) = c_0 + \frac{d}{r} + \frac{c_0^2 - 1}{3d}r - \frac{1}{3}\Lambda r^2. \quad (5)$$

It is clear that for nonvanishing Λ , Eq. (5) is not a solution of Einstein gravity, while as long as $\Lambda = 0$, the metric becomes identical to the Schwarzschild solution of Einstein gravity. It is worth mentioning that although Λ plays the role of the cosmological constant, it is arisen purely as an integration constant and is not put in the action by hand. Such a constant cannot be added to the action of CG because it would introduce a length scale and hence break the conformal invariance.

In order to add an action of matter, we should take care of its conformal transformation to keep the theory be conformally invariant. Fortunately, the Lagrangian of Maxwell theory is conformal invariant in four dimensions and we can add it to the gravitational sector of conformal theory as an appropriate matter field.

So, we can consider the static charged adS solutions of conformal- $U(1)$ gravity in four dimensions [13]. The appropriate action is

$$I = \alpha \int d^4x \sqrt{-g} \left(\frac{1}{2} C^{\mu\nu\rho\sigma} C_{\mu\nu\rho\sigma} + \frac{1}{3} F^{\mu\nu} F_{\mu\nu} \right), \quad (6)$$

where the unusual sign in front of the Maxwell term comes from the so-called critical gravity, which is necessary to recover the Einstein gravity from conformal gravity in IR limit. The static topological solution is found in [45] the same as Eq. (5) with the following gauge potential one form

$$A = -\frac{Q}{r} dt, \quad (7)$$

which leads to the following metric function [45]

$$f(r) = c_0 + \frac{d}{r} + c_1 r - \frac{1}{3}\Lambda r^2, \quad (8)$$

In order to have consistent solutions, three integration constants c_0 , c_1 , and d should obey an algebraic constraint

$$3c_1 d + \varepsilon^2 + Q^2 = c_0^2, \quad (9)$$

where $\varepsilon = 1, -1, 0$ denotes spherical, hyperbolic, and planar horizons, respectively. Therefore, the metric function takes the following compact form

$$f(r) = c_0 + \frac{d}{r} + \frac{c_0^2 - \varepsilon^2 - Q^2}{3d}r - \frac{1}{3}\Lambda r^2. \quad (10)$$

III. HIGHER DIMENSIONAL SOLUTIONS

Here, we are going to generalize the conformal action of $U(1)$ -gauge/gravity coupling in higher dimensions. As we know, the Maxwell action does not enjoy the conformal invariance properties in higher dimensions, and therefore, the higher dimensional solutions in CG cannot be produced in the presence of Maxwell field (and also the other electrodynamic fields that are not conformal invariant in higher dimensions). So, we should consider a generalization of linear Maxwell action to the case that it respects the invariance of conformal transformation. To do so, we take into account the power Maxwell nonlinear theory, which its Lagrangian is a power of Maxwell invariant, $(-F_{\mu\nu}F^{\mu\nu})^s$. It is a matter of calculation to show that the power Maxwell action enjoys the conformal invariance, for $s = D/4$ (D = dimension of spacetime) [46]. In other words, it is easy to show that as long as $s = D/4$, the energy-momentum tensor of power Maxwell invariant theory is traceless [46].

Regarding the mentioned issues, we find that the suitable action of higher dimensional conformal $U(1)$ -gauge/gravity action can be written as

$$I = \frac{1}{16\pi} \int d^D x \sqrt{-g} \left(C^{\mu\nu\rho\sigma} C_{\mu\nu\rho\sigma} + \beta (-F^{\mu\nu}F_{\mu\nu})^{\frac{D}{4}} \right). \quad (11)$$

Hereafter, we can regard a higher dimensional static spacetime and look for exact solutions with black hole interpretation. Variation of this action with respect to the metric tensor $g_{\mu\nu}$ and the Faraday tensor $F_{\mu\nu}$ leads to the following field equations

$$\mathbf{E}_{\rho\sigma} = \left(\nabla^\mu \nabla^\nu + \frac{1}{2} R^{\mu\nu} \right) C_{\rho\nu\mu\sigma} + \frac{\beta}{8} \left[g_{\rho\sigma} (-F^{\mu\nu}F_{\mu\nu})^{\frac{D}{4}} + D (-F^{\mu\nu}F_{\mu\nu})^{\frac{D}{4}-1} F_{\sigma\delta} F_\rho^\delta \right] = 0, \quad (12)$$

$$\partial_\rho \left[\sqrt{-g} (-F^{\mu\nu}F_{\mu\nu})^{\frac{D}{4}-1} F^{\rho\sigma} \right] = 0. \quad (13)$$

Since we are looking for topological black hole solutions of mentioned field equations, we express the metric of a D -dimensional spacetime as follows

$$ds^2 = -f(r)dt^2 + f^{-1}(r)dr^2 + r^2 d\Sigma_{k,D-2}^2, \quad (14)$$

where k denotes spherical ($k = 1$), hyperbolic ($k = -1$), and planar ($k = 0$) horizons of the $(D-2)$ -dimensional manifold with the following line element

$$d\Sigma_{k,D-2}^2 = \begin{cases} d\Omega_{D-2}^2 = d\theta_1^2 + \sum_{i=2}^{D-2} \prod_{j=1}^{i-1} \sin^2 \theta_j d\theta_i^2 & k = 1 \\ d\Xi_{D-2}^2 = d\theta_1^2 + \sinh^2 \theta_1 \left(d\theta_2^2 + \sum_{i=3}^{D-2} \prod_{j=2}^{i-1} \sin^2 \theta_j d\theta_i^2 \right) & k = -1 \\ dl_{D-2}^2 = \sum_{i=1}^{D-2} d\theta_i^2 & k = 0 \end{cases}, \quad (15)$$

in which $d\Omega_{D-2}^2$ is the standard metric of a unit $(D-2)$ -sphere, $d\Xi_{D-2}^2$ is the metric of a $(D-2)$ -dimensional hyperbolic plane with unit curvature, and dl_{D-2}^2 is the flat metric of R^{D-2} .

Using this metric and a radial gauge potential ansatz $A_\mu = -qr^{(2s-D+1)/(2s-1)}\delta_\mu^0$, one can find the nonzero components of the theory as follows

$$\begin{aligned} \mathbf{E}_{tt} = & 2D_3r^4f(r)f^{(4)}(r) + D_3[r f'(r) + 4D_{5/2}f(r)]r^3f'''(r) \\ & + \left[\frac{D_3}{2}r^2f''(r) + (2D^2D_{23/2} + 85D_{102/85})f(r) + D_3D_4\left(\frac{3rf'(r)}{2} + k\right) \right]r^2f''(r) \\ & - [3D_{10/3}D_3rf'(r) + (4D^2D_{49/4} + 187D_{228/187})f(r) + 5kD_3D_{16/5}]rf'(r) \\ & + 2(2D^2D_{23/2} + 84D_{99/84})f^2(r) - 4k(D^2D_{12} + 45D_{54/45})f(r) - 2D_3^2k^2 \\ & - \frac{D_1}{2}r^4\beta(1-2s)\left(\frac{\sqrt{2}q(2s-D_1)}{(2s-1)r^{(D-2)/(2s-1)}}\right)^{2s}, \end{aligned} \quad (16)$$

$$\begin{aligned} \mathbf{E}_{rr} = & D_3[2f(r) - rf'(r)]r^3f'''(r) - D_3\left[\frac{r^2}{2}f''(r) - 3D_{10/3}f(r) + D_4\left(\frac{3}{2}rf'(r) + k\right)\right] \\ & \times r^2f''(r) + D_3[3D_{10/3}rf'(r) - 9D_{28/9}f(r) + 5kD_{16/5}]rf'(r) \\ & + 2D_3^2[3f^2(r) - 4kf(r) + k^2] + \frac{D_1}{2}r^4\beta(1-2s)\left(\frac{\sqrt{2}q(2s-D_1)}{(2s-1)r^{(D-2)/(2s-1)}}\right)^{2s}, \end{aligned} \quad (17)$$

$$\begin{aligned} \mathbf{E}_{\theta\theta} = & D_3r^4f(r)f^{(4)}(r) + D_3[r f'(r) + 2D_3f(r)]r^3f'''(r) \\ & + \left[\frac{D_3}{2}r^2f''(r) + (D^2D_{13} + 52D_{66/52})f(r) + D_3D_4\left(\frac{3rf'(r)}{2} + k\right) \right]r^2f''(r) \\ & - [3D_{10/3}D_3rf'(r) + (2D^2D_{29/2} + 121D_{156/121})f(r) + 5kD_3D_{16/5}]rf'(r) \\ & + 2(D^2D_{13} + 51D_{63/51})f^2(r) - 2k(D^2D_{14} + 57D_{72/57})f(r) - 2D_3^2k^2 \\ & + \frac{D_1D_2}{4}r^4\beta\left(\frac{\sqrt{2}q(2s-D_1)}{(2s-1)r^{(D-2)/(2s-1)}}\right)^{2s}, \end{aligned} \quad (18)$$

in which we used $D_i = D - i$ for convenience and prime refers to d/dr . However, we will use common $D - i$ in indices and powers for clarity of equations. Solving Eqs. (16)-(18), and keeping in mind that $s = D/4$, we can obtain the metric function for $D \geq 5$ as follows

$$f(r) = k - \frac{C_1}{r^{D-3}} - \frac{\beta\mu q^{D/2}}{C_1}r + C_2r^2, \quad (19)$$

where C_1 and C_2 are two integration constants, and $\mu = 2^{(D-4)/4}(D_2D_3)^{-1}$ is a dimensionful constant. Interestingly, we see that although the field equations are too complicated, the solutions are quite simple. It is noticeable to mention that the solution to $D = 4$ is given by (10) when we set $\beta = -2/3$ in (11), but it cannot be obtained by using the field equations (16)-(18). Therefore, the four-dimensional spacetime has one more integration constant compared to the other dimensions.

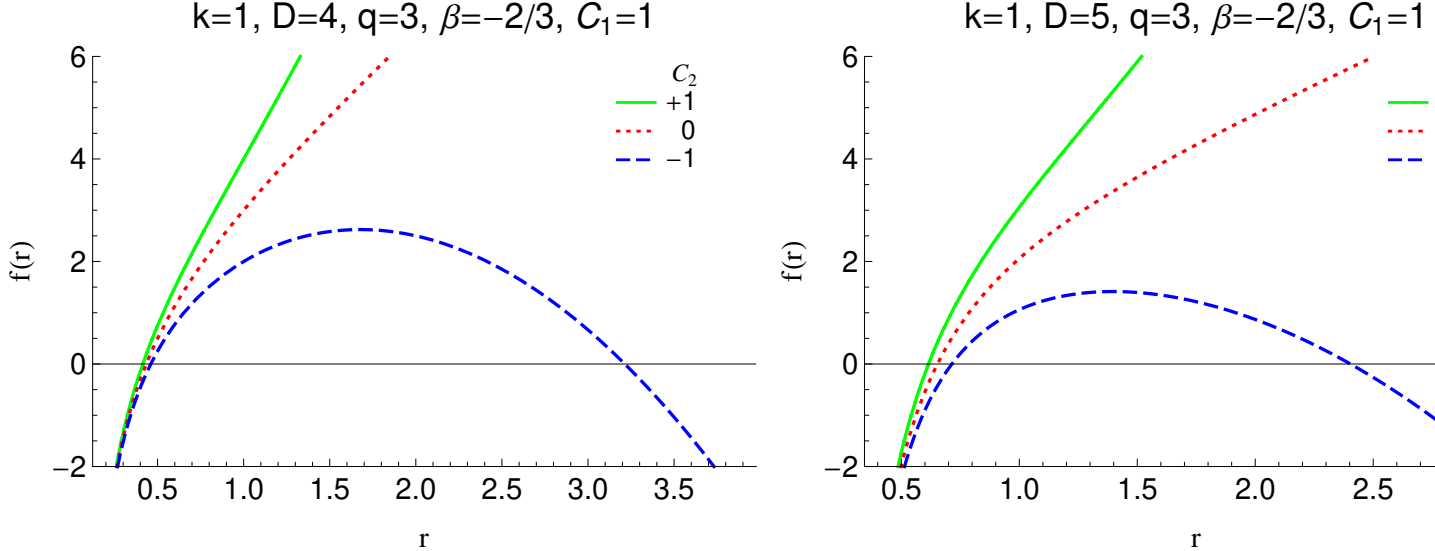


FIG. 1: The metric function versus radial coordinate. Positive C_2 corresponds to asymptotic adS solutions whereas the negative sign belongs to dS ones. In addition, for zero value of this parameter, the asymptotic behavior of these solutions are neither flat nor (a)dS. This is correct until the factor of r in the metric function (19) is a nonzero value.

In order to obtain a compact form of the metric function to be valid for all dimensions, one can consider a special case $c_0 = \varepsilon$ of the four-dimensional metric function (10). In this situation, the metric function of $D \geq 4$ is given by (19) and the field equations (16)-(18) can be used for $D = 4$ as well. We should note that since we considered a special case, $c_0 = \varepsilon$, the 4-dimensional solution given in (19) is also a solution of the field equations of (6).

Having solutions at hand, we are in a position to check that these solutions can be considered as a black hole or not. To do so, we first look for the singularities of the solutions. By calculating the Kretschmann scalar

$$R^{\lambda\tau\rho\sigma}R_{\lambda\tau\rho\sigma} = 2DD_1C_2^2 - \frac{4D_1D_2C_2\beta\mu q^{D/2}}{C_1r} + \frac{2D_2^2\beta^2\mu^2q^D}{C_1^2r^2} + \frac{D_1D_2^2D_3C_1^2}{r^{2(D-1)}}, \quad (20)$$

one can easily find that the metric (14) with the metric function (19) has an essential singularity at the origin ($\lim_{r \rightarrow 0} (R^{\lambda\tau\rho\sigma}R_{\lambda\tau\rho\sigma}) = \infty$). In addition, Fig. 1 shows that this singularity can be covered with an event horizon, and therefore, we can interpret the solution as a singular black hole.

IV. THERMODYNAMICS

A. Thermodynamic parameters

At this stage, we calculate temperature and entropy of the obtained solutions by using the surface gravity at the event horizon and the Wald entropy formula. Then, we will investigate thermal stability of black holes in the coming subsection.

By calculating the surface gravity, $\kappa = \sqrt{-(\nabla_\mu \chi_\nu)(\nabla^\mu \chi^\nu)/2}$ ($\chi = \partial_t$ is the null Killing vector of the horizon), we can obtain the Hawking temperature of the black hole at the outermost (event) horizon, r_+ . If we redefine (just for simplicity without loss of generality) the constants of the black hole solutions (19) as $C_1 \equiv m$, $\beta \mu q^{D/2}/C_1 \equiv \tilde{\mu}$, and $C_2 \equiv -\Lambda/3$, the metric function takes the following form

$$f(r) = k - \frac{m}{r^{D-3}} - \tilde{\mu}r - \frac{\Lambda}{3}r^2, \quad (21)$$

and accordingly, the temperature of the black hole is given as

$$T = \frac{\kappa}{2\pi} = \frac{f'(r)}{4\pi} \Big|_{r=r_+} = \frac{1}{12\pi r_+} (3D_3k - 3D_2\tilde{\mu}r_+ - D_1\Lambda r_+^2). \quad (22)$$

In addition, the entropy of the black hole in higher derivative theories can be obtained by Wald formula [47, 48] which makes the dependence of entropy on gravitational action

$$S = -2\pi \int_{\mathcal{M}} d^{D-2}x \sqrt{h} \frac{\delta \mathcal{L}}{\delta R_{\mu\nu\rho\sigma}} \xi_{\mu\nu} \xi_{\rho\sigma}, \quad (23)$$

where \mathcal{L} is the Lagrangian density of the theory, $\xi_{\mu\nu}$ is the binormal to the (arbitrary) cross-section \mathcal{M} of the horizon, and h is the determinant of induced volume on \mathcal{M} . Therefore, the entropy of our case study black hole takes the following form

$$S = -\frac{1}{8} \int_{\mathcal{M}} d^{D-2}x \sqrt{h} C^{\mu\nu\rho\sigma} \xi_{\mu\nu} \xi_{\rho\sigma} = \frac{D_2 D_3 m + \omega_{D-2}}{4r_+}, \quad (24)$$

in which ω_{D-2} denotes the volume of $d\Sigma_{k,D-2}^2$ and m_+ can be obtained by $f(r_+) = 0$. Here, we use the first law of thermodynamics ($\delta M = T\delta S$) to calculate the total mass of the solutions as

$$\begin{aligned} M = & \frac{\omega_{D-2} r_+^{D-5}}{144\pi D_4 D_5} \left\{ D_2 [3D_3 D_4 k (1 - \delta_{D,5})]^2 \right. \\ & - 3D_2 D_5 k [3D_3 \tilde{\mu} (17 + 2D D_6) (1 - \delta_{D,4}) + 2D_4 \Lambda (5 + D D_5) r_+] r_+ \\ & + D_3 D_4 D_5 \left[(3D_2 \tilde{\mu})^2 + 3\Lambda \tilde{\mu} (7 + 2D D_4) r_+ + (D_2 \Lambda r_+)^2 \right] r_+^2 \\ & \left. - 18D_5 k \ln \left(\frac{r_+}{l} \right) (D_4 \tilde{\mu} r_+ \delta_{D,4} - 6k \delta_{D,5}) \right\}, \end{aligned} \quad (25)$$

where $\delta_{a,b}$ is the Kronecker delta and l is a constant with length dimension.

Now, it is worthwhile to compare the neutral case ($\tilde{\mu} = 0$) of obtained solutions (21) with the (a)dS Schwarzschild black hole. The metric function and temperature are totally the same as the Schwarzschild one. But they have the same entropy just for $\Lambda = 3(D_2 D_3 r_+^2)^{-1} (6k + D D_5 k - r_+^2)$. In addition, one can solve $M - (48\pi)^{-1} D_1 r_+^{D-3} (3k - \Lambda r_+^2) = 0$ to find some conditions in order to have the same mass. However, we should note that it is not possible to find a constraint for conformal solutions to obtain the same entropy and mass of the Schwarzschild black hole, simultaneously.

B. Thermal stability

Now, we investigate the heat capacity of constructed black hole solutions in order to find the thermally stable criteria. The heat capacity of the solutions has the following explicit form

$$C = T \partial_T S = \frac{D_2 D_3 \omega_{D-2} r_+^{D-4} [3D_4 k - (3D_3 \tilde{\mu} + D_2 \Lambda r_+) r_+] [-3D_3 k + (3D_2 \tilde{\mu} + D_1 \Lambda r_+) r_+]}{12 (3D_3 k + D_1 \Lambda r_+^2)}. \quad (26)$$

The sign of heat capacity shows the stability condition of the solutions. The positive sign shows stable solutions whereas the negative sign indicates unstable ones. The heat capacity changes sign whenever it meets root or divergence points. The root of heat capacity indicates a bound point which separates the physical black holes (with positive temperature) from non-physical ones (with negative temperature). Moreover, divergence points may separate stable and unstable regions. Therefore, it is important to look for the roots and divergencies of Eq. (26). This equation has one divergence point (dp) given by

$$r_{+,dp} = \sqrt{-\frac{3D_3 k}{D_1 \Lambda}}, \quad (27)$$

which is real whenever k or Λ be negative. Thus, the heat capacity has, at most, one possible divergence point under certain conditions. As a result, the obtained black hole solutions just can undergo the Hawking-Page phase transition [49]. The root points (rp) of the heat capacity are

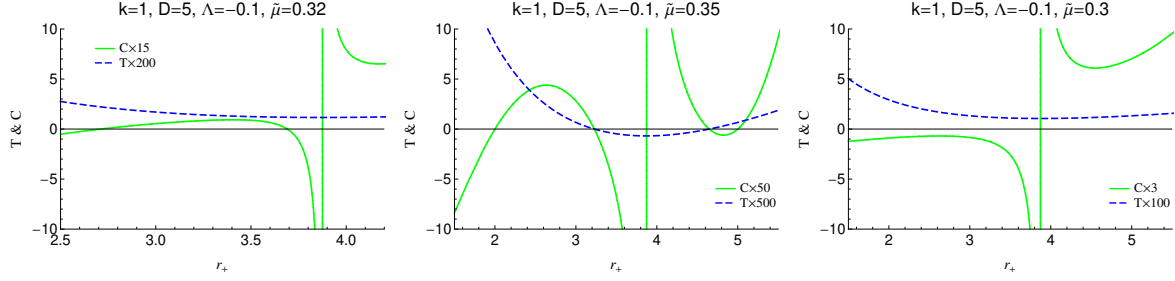


FIG. 2: *Spherical topology*: the heat capacity and temperature versus the event horizon radius for asymptotically adS black holes.

given by

$$r_{+,rp} = \begin{cases} r_{+,rp1} = -\frac{3D_3\tilde{\mu} + \sqrt{12D_2D_4k\Lambda + (3D_3\tilde{\mu})^2}}{2D_2\Lambda} \\ r_{+,rp2} = -\frac{3D_3\tilde{\mu} - \sqrt{12D_2D_4k\Lambda + (3D_3\tilde{\mu})^2}}{2D_2\Lambda} \\ r_{+,rp3} = -\frac{3D_2\tilde{\mu} + \sqrt{12D_1D_3k\Lambda + (3D_2\tilde{\mu})^2}}{2D_1\Lambda} \\ r_{+,rp4} = -\frac{3D_2\tilde{\mu} - \sqrt{12D_1D_3k\Lambda + (3D_2\tilde{\mu})^2}}{2D_1\Lambda} \end{cases}. \quad (28)$$

It is clear that the final number of real positive roots depends on the choice of the free parameters D , k , Λ , and $\tilde{\mu}$. For example, in order to have all four roots in adS spacetime, the free parameters should obey the certain condition $-\tilde{\mu}^2 \leq \frac{4D_1D_3k\Lambda}{3D_2^2} < 0$. This is the strongest condition on (28) which leads to four real positive roots for the heat capacity and there are some weaker conditions that lead to one, two or three roots. It is worthwhile to mention that due to the presence of more than one free parameter, we should fix some of them and study the conditions of appearing the roots and divergence point. However, this investigation is not enough to study the thermal stability of black holes and in order to see the positivity and negativity of the heat capacity, we should plot the related diagrams simultaneously. We do these studies for $\omega_{D-2} = 1$ and $\tilde{\mu} > 0$ as follows.

1. Case I: spherical topology ($k = 1$)

Here, we fix $k = 1$ and study the possibility of the presence of roots and divergence. At the same time, one may think about the asymptotic adS ($\Lambda < 0$) or dS ($\Lambda > 0$) solutions. For adS solutions, we have two roots given by $r_{+,rp1}$ and $r_{+,rp2}$ under condition $12D_2D_4\Lambda + (3D_3\tilde{\mu})^2 \geq 0$ (left panel of Fig. 2), and also, $r_{+,rp3}$ and $r_{+,rp4}$ for $12D_1D_3\Lambda + (3D_2\tilde{\mu})^2 \geq 0$ (middle panel of Fig.

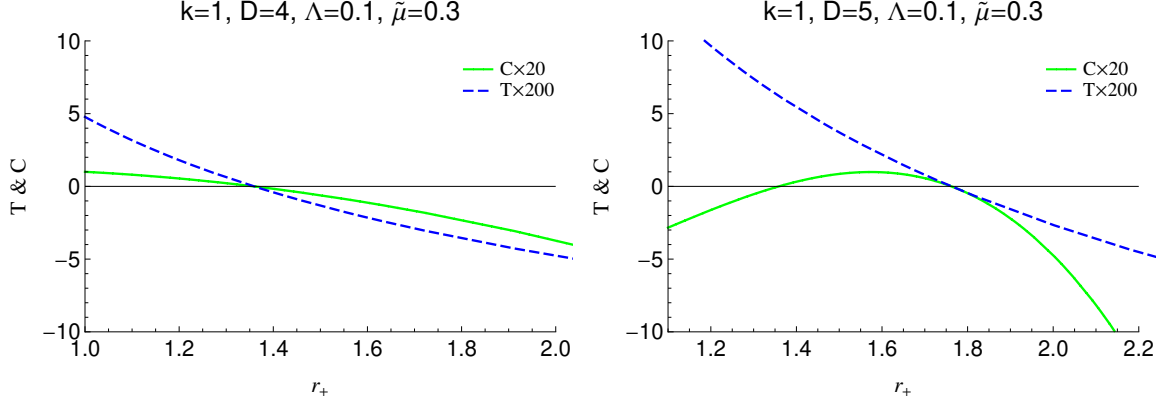


FIG. 3: *Spherical topology*: the heat capacity and temperature versus the event horizon radius for asymptotically dS black holes.

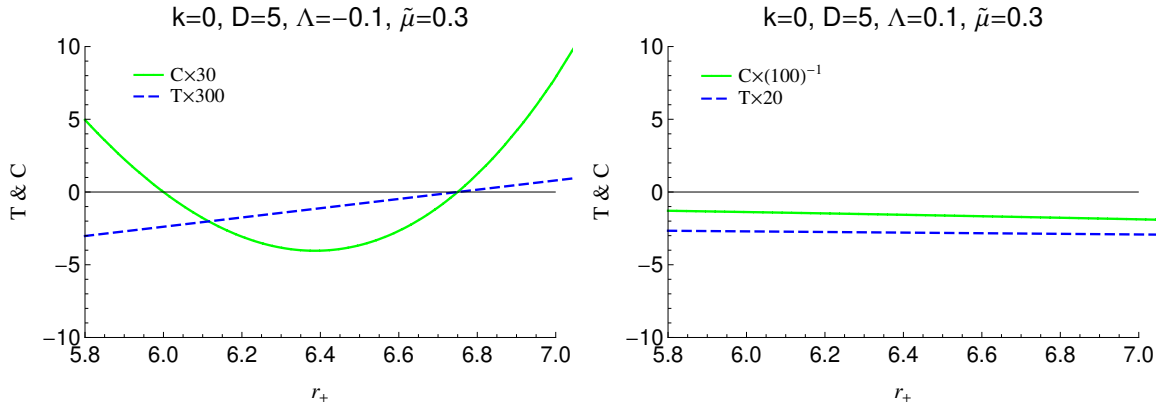


FIG. 4: *Flat topology*: the heat capacity and temperature versus the event horizon radius for asymptotically (a)dS black holes.

2). If we obey the stronger condition, $12D_1D_3\Lambda + (3D_2\tilde{\mu})^2 \geq 0$, all four roots will be appeared (middle panel of Fig. 2), and if we violate the weaker condition, $12D_2D_4\Lambda + (3D_3\tilde{\mu})^2 \geq 0$, there will be no root (right panel of Fig. 2). This is while the divergence point is always present.

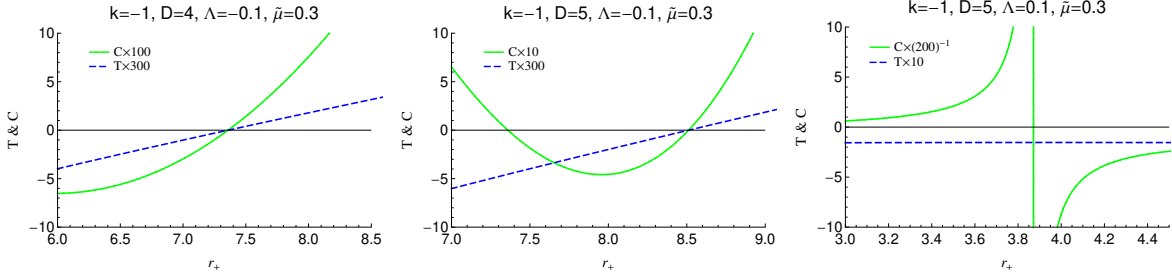


FIG. 5: *Hyperbolic topology*: the heat capacity and temperature versus the event horizon radius for asymptotically (a)dS black holes.

On the other hand, for dS solutions, there is no divergence point. In the case of roots, $r_{+,rp4}$ is always present (left panel of Fig. 3) and we have $r_{+,rp2}$ for $D > 4$ (right panel of Fig. 3). In both adS and dS cases, the behavior of the heat capacity and temperature is seen in Figs. 2 and 3. We recall that the positive sign of the heat capacity shows stable black holes and the negative sign indicates unstable ones. In addition, the positive (negative) temperature belongs to physical (non-physical) black holes.

Although we are dealing with some mathematical constraints, one should note that the obtained conditions and plotted diagrams tell us an important story about the existence possibility of obtained black holes. For example, we have physical and stable small black holes with spherical topology just in four dimensions with dS asymptote. On the other hand, the large black holes are always stable and physical in asymptotically adS spacetime.

2. Case II: flat topology ($k = 0$)

For $k = 0$, the divergence point will disappear and Eq. (28) reduces to $r_{+,rp1} = -3D_3\tilde{\mu}/(D_2\Lambda)$ and $r_{+,rp3} = -3D_2\tilde{\mu}/(D_1\Lambda)$. Therefore, there will be two roots for adS spacetime (left panel of Fig. 4) whereas there is no root for dS solutions (right panel of Fig. 4) which shows that dS black holes are unconditionally unstable and non-physical.

3. Case III: hyperbolic topology ($k = -1$)

Now, we set $k = -1$ and look for stable black holes in asymptotically adS spacetime. In this case, the divergence point is absent and there are always one root, $r_{+,rp3}$ (left panel of Fig. 5). For $D > 4$, $r_{+,rp1}$ will appear in addition to $r_{+,rp3}$ (middle panel of Fig. 5). For dS solutions, the divergence point will appear but there is no root (right panel of Fig. 5).

Although we presented our study for positive $\tilde{\mu}$, by considering $\tilde{\mu} = \beta\mu q^{D/2}/C_1$, $\tilde{\mu}$ can be negative whenever $D/2$ is an odd number and black hole has a negative net charge. This case is very interesting because the negative charge changes the spacetime geometry differently compared with a positive charge. However, since the negative charge of the black hole in some other dimensions leads to imaginary $\tilde{\mu}$ and this condition ($\tilde{\mu} < 0$) is a very special case, we do not involve it in our investigation. But, even considering this matter does not change our results significantly.

C. Possibility of critical behavior

Investigation of $P - V$ criticality of different types of black holes in thermodynamical extended phase space attracted attention during past decade (for instance, see an incomplete list [50–62] and references therein). The $P - V$ criticality of black holes is interesting because the black hole thermodynamics leads to very similar behavior as for the typical thermodynamic systems such as van der Waals fluid. In [63], it was shown that in order to observe the critical behavior for black holes, a local instability between two divergence points is required. Indeed, this local instability leads to a non-analytic behavior in the isotherm diagram which results in a small-large black hole phase transition. Since we have not seen such behavior (a local instability between two divergence points) during the thermal stability investigation (see Eq. (27)), our black hole case study cannot acquire the critical behavior with obtained temperature (22), entropy (24), and mass (25). Nevertheless, one can extend the thermodynamical phase space based on the Smarr relation into

$$M = \frac{2}{3}TS - \mathcal{V}\mathcal{P} + \Xi\tilde{\mu}, \quad (29)$$

where $\Xi = (\partial_{\tilde{\mu}}M)_{S,\mathcal{P}}$, $\mathcal{V} = (\partial_{\Lambda}M/\partial_{\Lambda}\mathcal{P})_{S,\tilde{\mu}}$, and \mathcal{P} is given by

$$\mathcal{P}_{D=4} = \frac{\exp[-2\Lambda r_+^2/(k - 5\tilde{\mu}r_+)]}{[kr_+(9\tilde{\mu} + \Lambda r_+) - 5\tilde{\mu}r_+^2(3\tilde{\mu} + \Lambda r_+) - 3k^2]^{3(4k^2 + 3k\tilde{\mu}r_+ + 5\tilde{\mu}^2r_+^2)/(2k - 10\tilde{\mu}r_+)^2}}, \quad (30)$$

$$\mathcal{P}_{D=5} = \frac{-\exp[6x(12k + 143\tilde{\mu}r_+)\arctan[x(9k + 42\tilde{\mu}r_+ - 2\Lambda r_+^2)]]}{[18k^2(3\ln(r_+/l) - 2) + 9kr_+(10\tilde{\mu} - \Lambda r_+) - r_+^2(45\tilde{\mu} - \Lambda r_+)(3\tilde{\mu} + \Lambda r_+)]^9}, \quad (31)$$

$$x = 3^{-1} [k^2(24\ln(r_+/l) - 25) - 4\tilde{\mu}r_+(11k + 64\tilde{\mu}r_+)]^{-1/2}, \quad (32)$$

and for $D \geq 6$, we have

$$\begin{aligned} \mathcal{P}_{D \geq 6} = & \left\{ r_+^{D-3} \left[D_2(3kD_3)^2 + D_3D_5r_+^2(3\tilde{\mu} + \Lambda r_+)(D_4\Lambda r_+ - 15D_2\tilde{\mu}) \right. \right. \\ & \left. \left. - 6D_5kr_+(\Lambda r_+(3 + DD_5) - 6D_3D_{5/2}\tilde{\mu}) \right] \right\}^{-3D_2/D_4} \times \\ & \exp \left[3D_2^{-1}D_4^{-1}\sqrt{D_5}\mathcal{X} [4D_2k(7 + DD_6) + 3D_3D_{4/3}\tilde{\mu}r_+(13 + 2DD_5)] \right. \\ & \left. \left. \arctan \left[3^{-1}\sqrt{D_5}\mathcal{X}(3k(3 + DD_5) + D_3r_+(6D_{3/2} - D_4\Lambda r_+)) \right] \right] \right], \end{aligned} \quad (33)$$

$$\mathcal{X} = \frac{1}{D_3\tilde{\mu}r_+} \left[\frac{k^2(219D_{57/73} + 8D^2D_{19/2})}{(D_3\tilde{\mu}r_+)^2} - D_5 \left(\frac{2k(51 + 6DD_{19/3})}{D_3\tilde{\mu}r_+} + 9D_{7/3}^2 \right) \right]^{-\frac{1}{2}}, \quad (34)$$

in which all the extensive and intensive parameters satisfy the first law of black hole thermodynamics as

$$dM = TdS + \mathcal{V}d\mathcal{P} + \Xi d\tilde{\mu}. \quad (35)$$

It is noticeable to mention that due to the presence of the Kronecker delta in mass parameter (25), we could not include $D = 4$ and 5 dimensions in (33). Now, it is worthwhile to concentrate our attention on the physical interpretation of P and V . At first glance and comparing (35) with modified first law of thermodynamics in the extended phase space calculated in [50–62], one may think that the pressure, $P = -\Lambda/8\pi$, modified into (30), (31), and (33) so that P and V be the thermodynamical pressure and volume. But these equations are dimensionless whereas the dimension of pressure is $(length)^{-2}$. Therefore, P and V cannot be considered as the thermodynamical pressure and volume of the system, and one can consider (35) just as a mathematical extension of the first law of thermodynamics at first step. However, the physical interpretation of P and V is arguable. This result confirms the fact that in order to have the critical behavior for black holes, a local instability between two divergencies in the heat capacity is required.

D. Geometrical thermodynamics

Geometrical thermodynamics is an interesting way to investigate the thermal stability of a thermodynamical system. In this perspective, the behavior of the system is governed by the Ricci scalar of a line element so that the components of the metric tensor field are the thermodynamic variables and their derivatives. In 1975, Weinhold [64, 65] introduced a line element on the space of equilibrium states which the metric components are the Hessian of internal energy. In addition, Ruppeiner and Quevedo have introduced two metrics in [66, 67] and [68, 69], respectively. Ruppeiner metric is conformally equivalent to Weinhold one whereas Quevedo metric enjoys the Legendre invariant and has been introduced to solve some problems in Weinhold and Ruppeiner metrics. Moreover, these three metrics were not free of shortcoming in the context of some black hole solutions [70]. Therefore, the fourth metric was introduced [70]

$$ds^2 = \frac{S\partial_S M}{\prod_{i=2} (\partial_{\chi_i}^2 M)^3} \left(-(\partial_S^2 M) dS^2 + \sum_{i=2} (\partial_{\chi_i}^2 M) d\chi_i^2 \right), \quad (36)$$

where χ_i 's are the residual extensive parameters with $\chi_i \neq S$. The geometrical thermodynamics of different types of black holes has been investigated in the literature [71–76] by using (36). Due to the complex values of \mathcal{P} and \mathcal{V} , we omit the term $\mathcal{V}d\mathcal{P}$ from the first law (35) and investigate the geometrical thermodynamics of the obtained solutions. For our black hole case study, the metric (36) reduces into

$$ds^2 = \frac{S\partial_S M}{(\partial_{\tilde{\mu}}^2 M)^3} \left[-(\partial_S^2 M) dS^2 + (\partial_{\tilde{\mu}}^2 M) d\tilde{\mu}^2 \right]. \quad (37)$$

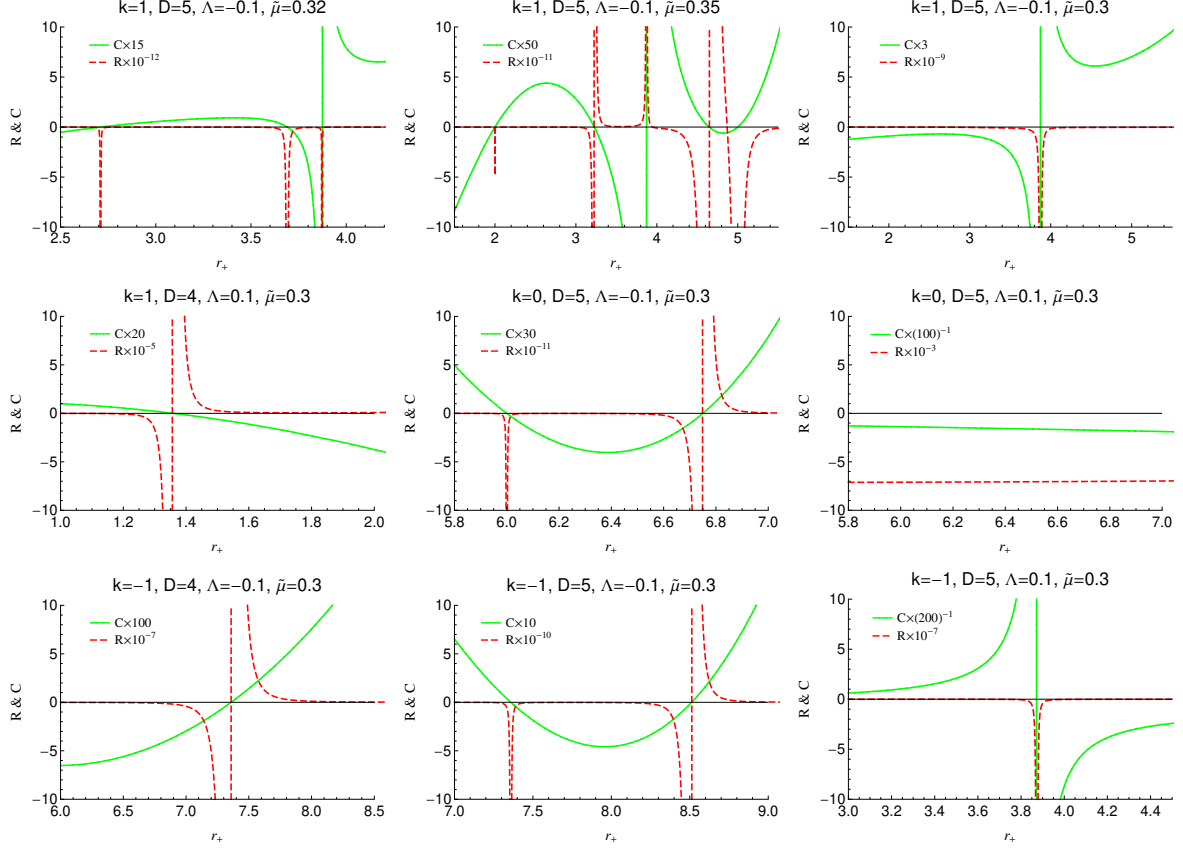


FIG. 6: The Ricci scalar and heat capacity versus the event horizon radius for Figs. 2-5.

Due to the cumbersome terms of the Ricci scalar (37), we do not show the explicit form of it for simplicity but the resulting diagrams are plotted in Fig. 6 related to the information of Figs. 2-5. From Fig. 6, interestingly, we can see that the singularities of the Ricci scalar totally coincide with all the points that the heat capacity changes sign, and more importantly, without introducing extra singular points.

V. QUASINORMAL MODES

A. Setup

Here, we consider a massive scalar perturbation in the background of the black hole spacetime and obtain the QNFs by using two independent methods of calculations; the sixth order WKB approximation [77–79] and the asymptotic iteration method (AIM) [80]. In addition, we concentrate our attention on the asymptotically dS black holes ($\Lambda > 0$) with spherical topology ($k = 1$) of the obtained metric function (21). The asymptotic flat solutions ($k = 1$, $\Lambda = 0$, and $\tilde{\mu} = 0$) reduce to

D -dimensional Schwarzschild black hole and one can use Horowitz-Hubeny method [21] to obtain the QNMs of asymptotically adS black holes ($\Lambda < 0$). A discussion on the adS black holes will appear elsewhere.

The equation of motion for a minimally coupled massive scalar field is given by

$$\square\Phi - \nu^2\Phi = 0, \quad (38)$$

so that ν is the mass of the scalar field Φ . If we consider modes

$$\Phi(t, r, \text{angles}) = r^{(2-D)/2}\Psi(r)Y(\text{angles})e^{-i\omega t}, \quad (39)$$

where $Y(\text{angles})$ denotes the spherical harmonics on $(D-2)$ -sphere, the equation of motion (38) reduces to the wavelike equation for the radial part $\Psi(r)$ in the following way

$$[\partial_x^2 + \omega^2 - V_l(x)]\Psi_l(x) = 0. \quad (40)$$

In this equation, x is the known tortoise coordinate with the definition

$$dx = \frac{dr}{f(r)}, \quad (41)$$

and the effective potential $V_l(x)$ is given by

$$V_l(x) = f(r) \left[\nu^2 + \frac{l(l+D-3)}{r^2} + \frac{(D-2)(D-4)}{4r^2}f(r) + \frac{D-2}{2r}f'(r) \right], \quad (42)$$

where l is the angular quantum number and note that r in the right-hand side is a function of x by (41). Figure 7 shows the behavior of this effective potential (42) versus the tortoise coordinate for some fixed values of different free parameters.

The spectrum of QNMs for a perturbed black hole spacetime is the solution of the wave equation (40). However, we have to impose some proper boundary conditions in order to obtain its solutions. The quasinormal boundary conditions imply that the wave at the event (cosmological) horizon is purely incoming (outgoing)

$$\begin{aligned} \Psi_l(r) &\sim e^{-i\omega x} & \text{as} & \quad x \rightarrow -\infty \quad (r \rightarrow r_e), \\ \Psi_l(r) &\sim e^{i\omega x} & \text{as} & \quad x \rightarrow \infty \quad (r \rightarrow r_c), \end{aligned} \quad (43)$$

where r_e is the event horizon and r_c is the cosmological horizon. One should consider the mentioned boundary conditions in order to obtain the QNFs.

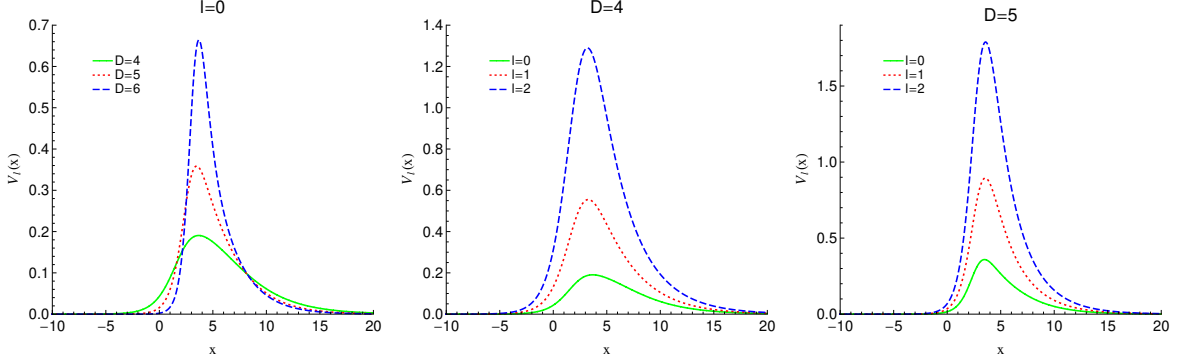


FIG. 7: Profiles of the effective potential for $m = 0.5$, $\tilde{\mu} = 0.3$, $\Lambda = 0.1$, and $\nu = 1$. The potential vanishes at both infinities.

B. WKB approximation

The method is based on the matching of WKB expansion of the wave function $\Psi_l(x)$ at the event horizon and cosmological horizon with the Taylor expansion near the peak of the potential barrier through the two turning points. Therefore, this method can be used for an effective potential that forms a potential barrier and takes constant values at the event horizon ($x \rightarrow -\infty$) and cosmological horizon ($x \rightarrow \infty$) (like Fig. 7). The WKB approximation was first applied to the problem of scattering around black holes [77], and then extended to the third order [78] and sixth order [79]. The WKB formula is given by

$$\frac{i(\omega^2 - V_0)}{\sqrt{-2V_0''}} - \sum_{j=2}^6 \Lambda_j = n + \frac{1}{2}; \quad n = 0, 1, 2, \dots, \quad (44)$$

where V_0 is the value of the effective potential at its local maximum, the correction terms Λ_j 's correspond to the j th order and depend on the value of the effective potential and its derivatives at the local maximum, and n is the overtone number. The explicit form of the WKB corrections is given in [78] (for Λ_2 and Λ_3) and [79] (for Λ_4 , Λ_5 , and Λ_6). It is worthwhile to mention that the WKB approximation does not give reliable frequencies for $n \geq l$. We use this formula up to the sixth order as a semi-analytical approach to obtain the QNFs of perturbation.

C. AIM

The AIM has been employed to solve the eigenvalue problems and solving second-order differential equations [81, 82], and then it was shown that it is an accurate technique for calculating QNMs [80, 83].

If one wants to employ the AIM, it is convenient to use the independent variable $\xi = 1/r$, and rewrite the wave equation (40) as

$$\frac{d^2\Psi_l(\xi)}{d\xi^2} + \frac{P'}{P} \frac{d\Psi_l(\xi)}{d\xi} + \left(\frac{\omega^2}{P^2} - \frac{V_l(\xi)}{P} \right) \Psi_l(\xi) = 0, \quad (45)$$

where P , P' , and $V_l(\xi)$ are given by

$$P = \xi^2 f(\xi); \quad f(\xi) = f(r)|_{r=1/\xi}, \quad (46)$$

$$P' = \frac{dP}{d\xi} = 2\xi - (D-1)m\xi^{D-2} - \tilde{\mu}, \quad (47)$$

$$V_l(\xi) = \left[\frac{\nu^2}{\xi^2} + l(l+D-3) + \frac{(D-2)(D-4)}{4} f(\xi) + \frac{D-2}{2\xi} f'(\xi) \right], \quad (48)$$

$$f'(\xi) = \left. \frac{df(r)}{dr} \right|_{r=1/\xi} = (D-3)m\xi^{D-2} - \tilde{\mu} - \frac{2\Lambda}{3\xi}. \quad (49)$$

In order to choose the appropriate scaling behavior for quasinormal boundary conditions, one may define [83, 84]

$$e^{i\omega x} = \prod_j (\xi - \xi_j)^{-i\omega/\kappa_j}, \quad (50)$$

in which κ_j is the surface gravity at ξ_j with $f(\xi = \xi_j) = 0$. This equation scale out the divergent behavior at some boundary ξ_j and applies the boundary conditions (43) to the solution.

Now, by redefinition of $\Psi_l(\xi)$ as

$$\Psi_l(\xi) = e^{i\omega x} \psi_l(\xi), \quad (51)$$

the equation (45) converts to

$$P \frac{d^2\psi_l(\xi)}{d\xi^2} + (P' - 2i\omega) \frac{d\psi_l(\xi)}{d\xi} - V_l(\xi) \psi_l(\xi) = 0. \quad (52)$$

Based on the equations (50) and (51), the correct quasinormal condition at the event horizon, ξ_e , is

$$\psi_l(\xi) = (\xi - \xi_e)^{-i\omega/\kappa_e} \mathcal{U}_l(\xi), \quad (53)$$

where

$$\kappa_e = \frac{1}{2} \left. \frac{df(r)}{dr} \right|_{r=r_e} = \frac{1}{2} f'(\xi_e). \quad (54)$$

By inserting (53) into (52), one can find the standard AIM form as follows

$$\frac{d^2\mathcal{U}_l(\xi)}{d\xi^2} = \lambda_0(\xi) \frac{d\mathcal{U}_l(\xi)}{d\xi} + s_0(\xi) \mathcal{U}_l(\xi), \quad (55)$$

so that $\lambda_0(\xi)$ and $s_0(\xi)$ are

$$\lambda_0(\xi) = -\frac{1}{P} \left(P' - 2i\omega - \frac{2i\omega P}{\kappa_e(\xi - \xi_e)} \right), \quad (56)$$

$$s_0(\xi) = \frac{1}{P} \left[\frac{i\omega(P' - 2i\omega)}{\kappa_e(\xi - \xi_e)} - \frac{i\omega P}{\kappa_e(\xi - \xi_e)^2} \left(\frac{i\omega}{\kappa_e} + 1 \right) + V_l(\xi) \right]. \quad (57)$$

We will use Eqs. (55)-(57) to calculate the QNFs as a numerical method for obtained black hole solutions in the coming section (see [80, 83] for details of calculations).

D. Time-domain profiles

Using the time-domain integration of the wavelike equation (40), one can study the contribution of all the modes for a fixed value of the angular quantum number in a single ringing profile. The time-domain profile of modes shows the behavior of the asymptotic tails after ringdown stage at late times. In order to obtain the time evolution of modes, we follow the discretization scheme given in [85] (see also [25] and [86]). In terms of the light-cone coordinates $u = t - x$ and $v = t + x$, the perturbation equation (40) takes the following form

$$[4\partial_u\partial_v + V_l(u, v)]\Psi_l(u, v) = 0. \quad (58)$$

By integrating the mentioned equation on the small grids on the two null surfaces $u = u_0$ and $v = v_0$ as the initial data, one can obtain the time-domain profile of modes. By applying the time evolution operator on $\Psi_l(u, v)$ and expanding this operator for sufficiently small grids, one can obtain the evolution equation in the light-cone coordinates as below

$$\begin{aligned} \Psi_l(u + \Delta, v + \Delta) = & \Psi_l(u + \Delta, v) + \Psi_l(u, v + \Delta) - \Psi_l(u, v) \\ & - \frac{\Delta^2}{8} [V_l(u + \Delta, v)\Psi_l(u + \Delta, v) + V_l(u, v + \Delta)\Psi_l(u, v + \Delta)], \end{aligned} \quad (59)$$

which Δ is the step size of the grids. We shall obtain the time evolution of perturbations with a Gaussian wave packet as initial data on the surfaces $u = u_0$ and $v = v_0$.

E. Results and discussion

The QNMs are calculated by using the sixth order WKB approximation and AIM after 15 iterations, and results are presented in tables *I – IV*. The tables contain the fundamental QNM ($n = 0$) for different values of spacetime dimension and multipole number, and fixed $m = 0.5$, $\tilde{\mu} = 0.3$, $\Lambda = 0.1$, and $\nu = 1$.

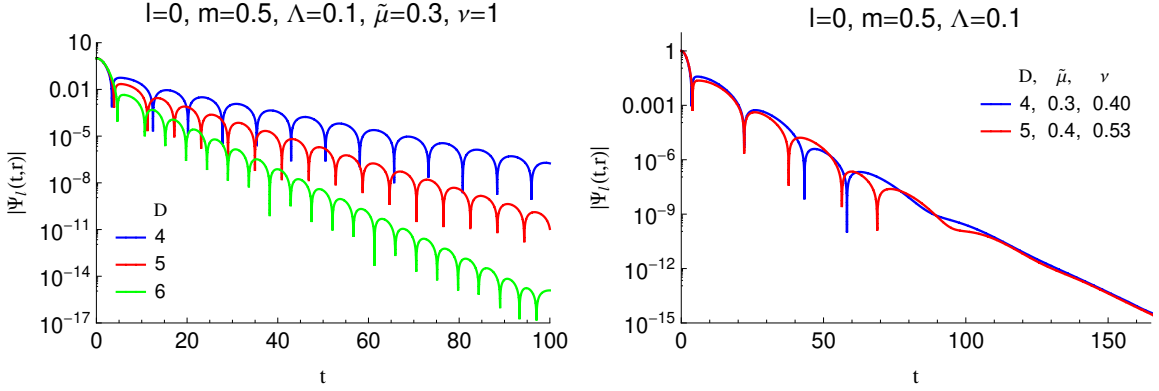


FIG. 8: The absolute value of the wave function $\Psi_l(t, r)$ versus time for the values of table *II* (left panel) and for some special values indicating the power law damping modes at late times (right panel).

From table *I*, we find that although the WKB approximation does not give reliable frequencies for $n \geq l$, for higher dimensions, say $D \geq 6$, the WKB formula gives better results for $n = 0 = l$. However, for a fixed multipole number so that $l \geq 1$, as the dimension increases, the result of WKB formula gets worse. In addition, most of the results of WKB approximation are in a good agreement with numeric results (tables *II* – *IV*), and results get better for the higher multipole number (for example, compare the row with $D = 7$ of tables *II* – *IV*), as we expected. On the other hand, both the real and imaginary parts of the QNFs increase with increasing in dimension which shows that there are more oscillations for higher dimensions at ringdown stage and the modes live longer for lower dimensions (see the left panel of Fig. 8).

On the other hand, as one can see from Fig. 7, the effective potential forms a potential barrier which is positive everywhere and vanishes at the event horizon and spatial infinity. This leads to the following fact

$$\int_{-\infty}^{+\infty} V_l(x) dx > 0, \quad (60)$$

which shows that we can find dynamically stable black holes under massive scalar perturbations from the obtained solutions [87]. The right panel of Fig. 8 indicates the late time behavior of modes. The power law decay of modes at late times confirms the fact that the black holes enjoy the dynamical stability.

In addition, it is worthwhile to mention that although the calculated QNMs in tables *I* – *IV* are related to the dynamically stable black holes under massive scalar perturbations, these black holes are thermally stable just in four dimensions. Therefore, the obtained black hole solutions in $D > 4$ are stable dynamically, but not thermally.

D	AIM ($\omega_r - i\omega_i$)	WKB ($\omega_r - i\omega_i$)	r_e
4	$0.41487 - 0.12777i$	$0.18614 - 1.4372i$ (55.13%, 1024.83%)	$0.62556 < r_{+,rp4}$
5	$0.52903 - 0.20231i$	$0.67709 - 0.10511i$ (27.99%, 48.05%)	$0.82840 < r_{+,rp2}$
6	$0.66789 - 0.32804i$	$0.67545 - 0.31549i$ (1.13%, 3.83%)	$0.89131 < r_{+,rp2}$
7	$0.86292 - 0.46763i$	$0.87357 - 0.46878i$ (1.23%, 0.25%)	$0.92081 < r_{+,rp2}$
8	$1.0886 - 0.58598i$	$1.0992 - 0.59847i$ (0.97%, 2.13%)	$0.93779 < r_{+,rp2}$
9	$1.3291 - 0.69027i$	$1.3383 - 0.71872i$ (0.69%, 4.12%)	$0.94880 < r_{+,rp2}$
10	$1.5801 - 0.78466i$	$1.5858 - 0.83505i$ (0.36%, 6.42%)	$0.95651 < r_{+,rp2}$

Table *I*: The fundamental QNM for $l = 0$. r_e shows the value of the event horizon radius for each dimension. For $D = 4$, the event horizon radius is smaller than the only root of the heat capacity $r_{+,rp4}$, and therefore, this black hole is thermally stable (see the left panel of Fig. 3). However, for other dimensions, the event horizon radius is located before the smaller root of the heat capacity $r_{+,rp2}$, and therefore, these black holes are thermally unstable (see the right panel of Fig. 3).

D	AIM ($\omega_r - i\omega_i$)	WKB ($\omega_r - i\omega_i$)
4	$0.71667 - 0.16408i$	$0.71680 - 0.16407i$ (0.02%, < 0.01%)
5	$0.89554 - 0.24159i$	$0.89528 - 0.24209i$ (0.03%, 0.21%)
6	$1.1454 - 0.34506i$	$1.1442 - 0.34700i$ (0.10%, 0.56%)
7	$1.4091 - 0.44882i$	$1.4055 - 0.45391i$ (0.26%, 1.13%)
8	$1.6807 - 0.54759i$	$1.6720 - 0.55880i$ (0.52%, 2.05%)
9	$1.9579 - 0.64053i$	$1.9400 - 0.66216i$ (0.91%, 3.38%)
10	$2.2397 - 0.72789i$	$2.2063 - 0.76562i$ (1.49%, 5.18%)

Table *II*: The fundamental QNM for $l = 1$.

D	AIM ($\omega_r - i\omega_i$)	WKB ($\omega_r - i\omega_i$)
4	$1.1161 - 0.17673i$	$1.1161 - 0.17673i$ (< 0.01%, < 0.01%)
5	$1.3025 - 0.25160i$	$1.3025 - 0.25162i$ (< 0.01%, < 0.01%)
6	$1.6110 - 0.34815i$	$1.6111 - 0.34813i$ (< 0.01%, < 0.01%)
7	$1.9262 - 0.44387i$	$1.9265 - 0.44361i$ (0.02%, 0.06%)
8	$2.2400 - 0.53549i$	$2.2411 - 0.53458i$ (0.05%, 0.17%)
9	$2.5524 - 0.62251i$	$2.5550 - 0.62037i$ (0.10%, 0.34%)
10	$2.8637 - 0.70509i$	$2.8690 - 0.70105i$ (0.19%, 0.57%)

Table *III*: The fundamental QNM for $l = 2$.

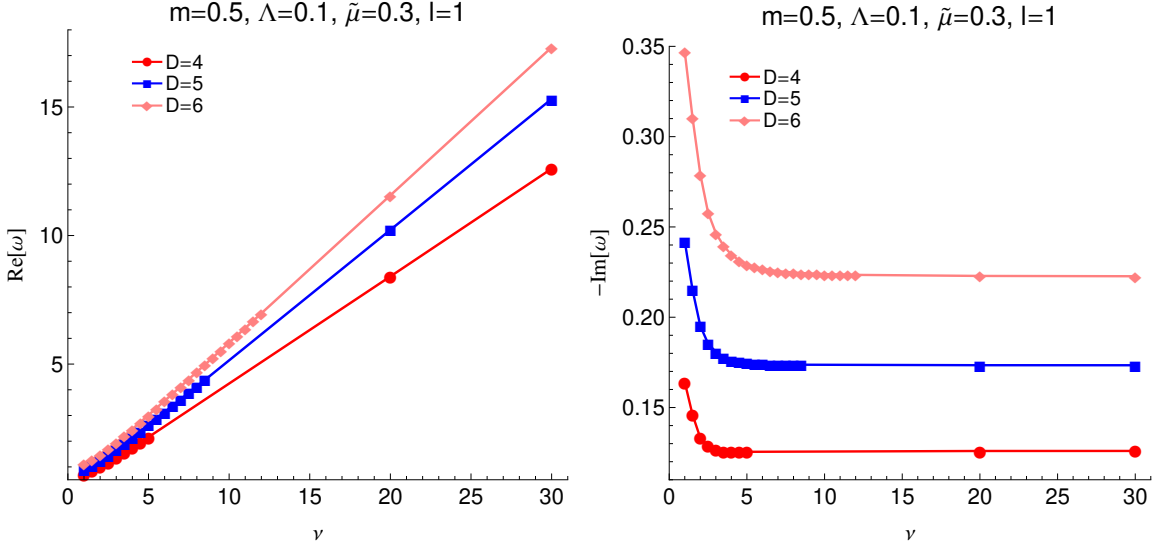


FIG. 9: The real and imaginary parts of fundamental QNMs as a function of scalar field mass calculated by using the WKB formula.

D	AIM ($\omega_r - i\omega_i$)	WKB ($\omega_r - i\omega_i$)
4	$1.5323 - 0.18053i$	$1.5323 - 0.18053i$ ($< 0.01\%, < 0.01\%$)
5	$1.7173 - 0.25513i$	$1.7173 - 0.25513i$ ($< 0.01\%, < 0.01\%$)
6	$2.0745 - 0.34934i$	$2.0745 - 0.34932i$ ($< 0.01\%, < 0.01\%$)
7	$2.4341 - 0.44183i$	$2.4342 - 0.44169i$ ($< 0.01\%, 0.03\%$)
8	$2.7857 - 0.53009i$	$2.7860 - 0.52960i$ ($0.01\%, 0.09\%$)
9	$3.1299 - 0.61393i$	$3.1309 - 0.61267i$ ($0.03\%, 0.21\%$)
10	$3.4686 - 0.69364i$	$3.4710 - 0.69094i$ ($0.07\%, 0.39\%$)

Table IV: The fundamental QNM for $l = 3$.

On the other hand, one of the motivations for considering the test massive fields comes from the fact that there are some QNMs with arbitrarily long life (purely real) modes called quasi-resonance modes [88]. For the quasi-resonance modes, the oscillations do not decay and the situation is similar to the standing waves on a string which is fixed at its both ends. The quasi-resonance modes occur for special values of field mass and the QNMs disappear when the field mass takes higher values. However, this happens just for lower overtones whenever the effective potential is non-zero at least at one of the boundaries (the event horizon $x \rightarrow -\infty$ or cosmological horizon $x \rightarrow \infty$).

Now, let us investigate the possibility of the quasi-resonance modes presence for obtained black hole solutions. The effective potential (42) vanishes at both infinities for all possible values of

different parameters, and therefore, there is no quasi-resonance modes for (40). In addition, if one sets the integration constant $-\Lambda/3$ equals to zero, the effective potential still vanishes at both infinities. There is only one case so that the effective potential can be non-zero at spatial infinity and that is neutral black holes ($\tilde{\mu} = 0$) with zero integration constant ($-\Lambda/3 = 0$). In this case, the effective potential reduces to the Schwarzschild one which its quasi-resonance modes have been investigated in [89]. Therefore, our black hole case study has no quasi-resonant oscillations in general and the imaginary part of the frequencies never vanishes. Figure 9 shows the behavior of QNFs with increasing in ν and confirms the above discussion. As ν increases, the real part of frequencies increases too, whereas the imaginary part first decreases rapidly and then takes a constant value.

VI. CONCLUSIONS

Motivated by the importance of higher dimensional spacetime in high energy physics, we have constructed the conformal- $U(1)$ gauge/gravity black hole solutions in $D \geq 4$. Since higher-dimensional solutions in CG cannot be produced in the presence of Maxwell field (and also the other electrodynamic fields that are not conformal invariant in higher dimensions), we have used a class of nonlinear electrodynamics $(-F_{\mu\nu}F^{\mu\nu})^s$ (which enjoys the conformal invariance properties in higher dimensions as $s = D/4$) to obtain black hole solutions. In addition, we have seen that the obtained solutions enjoy an essential singularity at the origin and they can be considered as black holes.

We have calculated the conserved charges of the obtained black hole solutions and studied the thermal stability of these black holes in the canonical ensemble. We have calculated the root and divergence points of the heat capacity and obtained some regions where the black holes are stable and physical. It was shown that the large black holes are always physical and stable in adS spacetime whereas these black holes are unconditionally unstable and non-physical in arbitrary dimensional dS spacetime. We have also investigated the thermal stability with geometrical thermodynamics approach and we have seen that the singularities of the Ricci scalar totally coincide with all points that the heat capacity changes sign without introducing extra singular points. Then, we have shown that the obtained black hole solutions cannot undergo the van der Waals like phase transition because of the absence of local instability.

Furthermore, we have considered a minimally coupled massive scalar perturbation in the background spacetime of our the black hole case study and calculated the QNFs by using the sixth

order WKB approximation and the AIM after 15 iterations. We also investigated the time evolution of modes in some diagrams. We have shown that although the WKB approximation does not give reliable frequencies for $n \geq l$, this approximation gives better results in higher dimensions for $n = 0 = l$. It was shown that most of the results of WKB approximation are in a good agreement with AIM and results get better for the higher multipole number. Besides, we observed that there were more oscillations for higher dimensions and the modes live longer for lower dimensions. We also showed that the four-dimensional black holes are stable both thermally and dynamically. However, the higher dimensional black holes were thermally unstable but they enjoy the dynamical stability. We should note that the previous results have been obtained for some special values of free parameters and it may be possible to find stable black holes in higher dimensions by choosing some other values for the free parameters. In addition, we argued that the black holes have no quasi-resonant oscillations even when one sets the integration constant $-\Lambda/3$ equals to zero. This happens due to the presence of the linear r -term. Therefore, the imaginary part of the frequencies never vanishes and there are always damping modes (QNFs are always complex).

Here, we finish our paper with some suggestions. One can consider (minimally or non-minimally coupled) the other kinds of perturbations such as charged scalar perturbation, electromagnetic perturbation, Proca field, and etc on the background spacetime of these black holes and calculate the QNFs and investigate the dynamical stability. Investigating the near extremal regime of these black holes in dS spacetime is an interesting work which is under examination.

Acknowledgments

We wish to thank Shiraz University Research Council. MM wishes to thank A. Zhidenko and R. A. Konoplya for their helps on QNMs. This work has been supported financially by the Research Institute for Astronomy and Astrophysics of Maragha, Iran.

- [1] R. J. Riegert, Phys. Rev. Lett. 53 (1984) 315.
- [2] H. Lu and C. N. Pope, Phys. Rev. Lett. 106 (2011) 181302.
- [3] E. Bergshoeff, M. de Roo and B. de Wit, Nucl. Phys. B 182 (1981) 173.
- [4] B. de Wit, J. W. van Holten and A. Van Proeyen, Nucl. Phys. B 184 (1981) 77.
- [5] S. L. Adler, Rev. Mod. Phys. 54 (1982) 729.
- [6] G. 't Hooft, Found. Phys. 41 (2011) 1829.
- [7] P. D. Mannheim, Found. Phys. 42 (2012) 388.

- [8] N. Berkovits and E. Witten, JHEP 08 (2004) 009.
- [9] H. Liu and A. A. Tseytlin, Nucl. Phys. B 533 (1998) 88.
- [10] V. Balasubramanian, E. G. Gimon, D. Minic and J. Rahmfeld, Phys. Rev. D 63 (2001) 104009.
- [11] K. S. Stelle, Phys. Rev. D 16 (1977) 953.
- [12] B. Hasslacher and E. Mottola, Phys. Lett. B 99 (1981) 221.
- [13] R. Bach, Math. Z. 9 (1921) 110.
- [14] A. Buchdahl, Edinburgh Math. Soc. Proc. 10 (1953) 16.
- [15] J. Maldacena, [arXiv:1105.5632].
- [16] G. Anastasiou and R. Olea, Phys. Rev. D 94 (2016) 086008.
- [17] S. Deser, H. Liu, H. Lu, C. N. Pope, T. C. Sisman and B. Tekin, Phys. Rev. D 83 (2001) 061502.
- [18] C. Lanczos, Annals Math. 39 (1938) 842.
- [19] H. Nollert, Phys. Rev. D 47 (1993) 5253.
- [20] S. Hod, Phys. Rev. Lett. 81 (1998) 4293.
- [21] G. T. Horowitz and V. E. Hubeny, Phys. Rev. D 62 (2000) 024027.
- [22] V. Cardoso and J. P. S. Lemos, Phys. Rev. D 64 (2001) 084017.
- [23] K. D. Kokkotas and B. G. Schmidt, Living Rev. Rel. 2 (1999) 2.
- [24] E. Berti, V. Cardoso and A. O. Starinets, Class. Quant. Grav. 26 (2009) 163001.
- [25] R. A. Konoplya and A. Zhidenko, Rev. Mod. Phys. 83 (2011) 793.
- [26] B. P. Abbott et al. [LIGO Scientific and Virgo Collaborations], Phys. Rev. Lett. 116 (2016) 061102.
- [27] B. P. Abbott et al. [LIGO Scientific and Virgo Collaborations], Phys. Rev. Lett. 116 (2016) 221101.
- [28] B. P. Abbott et al. [LIGO Scientific and Virgo Collaborations], Phys. Rev. Lett. 116 (2016) 241103.
- [29] R. A. Konoplya and A. Zhidenko, JCAP 12 (2016) 043.
- [30] K. Lin, W. L. Qian and A. B. Pavan, Phys. Rev. D 94 (2016) 064050.
- [31] G. B. Cook and M. Zalutskiy, Phys. Rev. D 94 (2016) 104074.
- [32] N. Breton and L. A. Lopez, Phys. Rev. D 94 (2016) 104008.
- [33] P. A. Gonzalez, R. A. Konoplya and Y. Vasquez, Phys. Rev. D 95 (2017) 124012.
- [34] J. L. Blazquez-Salcedo, F. S. Khoo and J. Kunz, Phys. Rev. D 96 (2017) 064008.
- [35] K. Lin, W. L. Qian, A. B. Pavan and E. Abdalla, Mod. Phys. Lett. A 32 (2017) 1750134.
- [36] G. Khanna and R. H. Price, Phys. Rev. D 95 (2017) 081501.
- [37] M. Wang, C. Herdeiro and J. Jing, Phys. Rev. D 96 (2017) 104035.
- [38] R. A. Konoplya and A. Zhidenko, Phys. Rev. D 97 (2018) 084034.
- [39] V. Cardoso, J. L. Costa, K. Destounis, P. Hintz and A. Jansen, Phys. Rev. Lett. 120 (2018) 031103.
- [40] R. A. Konoplya, Z. Stuchlik and A. Zhidenko, Phys. Rev. D 98 (2018) 104033.
- [41] T. Assumpcao, V. Cardoso, A. Ishibashi, M. Richartz and M. Zilhao, Phys. Rev. D 98 (2018) 064036.
- [42] J. L. Blazquez-Salcedo, X. Y. Chew and J. Kunz, Phys. Rev. D 98 (2018) 044035.
- [43] K. Destounis, G. Panotopoulos and A. Rincon, [arXiv:1801.08955].
- [44] G. Panotopoulos, [arXiv:1807.03278].

- [45] J. Li, H. S. Liu, H. Lu and Z. L. Wang, JHEP 02 (2013) 109.
- [46] M. Hassaine and C. Martinez, Phys. Rev. D 75 (2007) 027502.
- [47] R. M. Wald, Phys. Rev. D 48 (1993) 3427.
- [48] V. Iyer and R. M. Wald, Phys. Rev. D 52 (1995) 4430.
- [49] S. Hawking and D. Page, Commun. Math. Phys. 87 (1983) 577.
- [50] D. Kubiznak and R. B. Mann, JHEP 07 (2012) 033.
- [51] M. B. J. Poshteh, B. Mirza and Z. Sherkatghanad, Phys. Rev. D 88 (2013) 024005.
- [52] E. Caceres, P. H. Nguyen and J. F. Pedraza, JHEP 09 (2015) 184.
- [53] S. H. Hendi, S. Panahiyan, B. Eslam Panah, M. Faizal and M. Momennia, Phys. Rev. D 94 (2016) 024028.
- [54] A. Mandal, S. Samanta and B. R. Majhi, Phys. Rev. D 94 (2016) 064069.
- [55] S. H. Hendi, S. Panahiyan and M. Momennia, Int. J. Mod. Phys. D 25 (2016) 1650063.
- [56] R. A. Hennigar, E. Tjoab and R. B. Mann, JHEP 02 (2017) 070.
- [57] S. H. Hendi and M. Momennia, Eur. Phys. J. C 78 (2018) 800.
- [58] S. H. Hendi and M. Momennia, Phys. Lett. B 777 (2018) 222.
- [59] A. Ovgun, Adv. High Energy Phys. 2018 (2018) 8153721.
- [60] Z. Sun and M. S. Ma, EPL 122 (2018) 60002.
- [61] B. Liu, Z. Y. Yang and R. H. Yue, [arXiv:1810.07885].
- [62] M. Jamil, B. Pourhassan, A. Ovgun and I. Sakalli, [arXiv:1811.02193].
- [63] S. H. Hendi and M. Momennia, [arXiv:1801.07906].
- [64] F. Weinhold, J. Chem. Phys. 63 (1975) 2479.
- [65] F. Weinhold, J. Chem. Phys. 63 (1975) 2484.
- [66] G. Ruppeiner, Phys. Rev. A 20 (1979) 1608.
- [67] G. Ruppeiner, Rev. Mod. Phys. 67 (1995) 605.
- [68] H. Quevedo, J. Math. Phys. 48 (2007) 013506.
- [69] H. Quevedo, A. Sanchez, JHEP 09 (2008) 034.
- [70] S. H. Hendi, S. Panahiyan, B. Eslam Panah and M. Momennia, Eur. Phys. J. C 75 (2015) 507.
- [71] M. Chabab, H. El Moumni and K. Masmar, Eur. Phys. J. C 76 (2016) 304.
- [72] S. H. Hendi, S. Panahiyan, M. Momennia and B. Eslam Panah, Int. J. Mod. Phys. D 26 (2017) 1750026.
- [73] M. Zhang, Nucl. Phys. B 935 (2018) 170.
- [74] M. Zhang and W. B. Liu, [arXiv:1610.03648].
- [75] Kh. Jafarzade and J. Sadeghi, [arXiv:1711.04522].
- [76] T. Vetsov, [arXiv:1806.05011].
- [77] B. F. Schutz and C. M. Will, Astrophys. J. Lett. 291 (1985) L33.
- [78] S. Iyer and C. M. Will, Phys. Rev. D 35 (1987) 3621.
- [79] R. A. Konoplya, Phys. Rev. D 68 (2003) 024018.
- [80] H. T. Cho, A. S. Cornell, J. Doukas, T. R. Huang and W. Naylor, Adv. Math. Phys. 2012 (2012)

281705.

- [81] H. Ciftci, R. L. Hall and N. Saad, *J. Phys. A* 36 (2003) 11807.
- [82] H. Ciftci, R. L. Hall and N. Saad, *Phys. Lett. A* 340 (2005) 388.
- [83] H. T. Cho, A. S. Cornell, J. Doukas and W. Naylor, *Class. Quant. Grav.* 27 (2010) 155004.
- [84] I. G. Moss and J. P. Norman, *Class. Quant. Grav.* 19 (2002) 2323.
- [85] C. Gundlach, R. H. Price and J. Pullin, *Phys. Rev. D* 49 (1994) 883.
- [86] S. Chakraborty, K. Chakravarti, S. Bose and S. SenGupta, *Phys. Rev. D* 97 (2018) 104053.
- [87] B. Simon, *Ann. Phys.* 97 (1976) 279.
- [88] A. Ohashi and M. a. Sakagami, *Class. Quant. Grav.* 21 (2004) 3973.
- [89] R. A. Konoplya and A. Zhidenko, *Phys. Lett. B* 609 (2005) 377.